Solar Energy Materials & Solar Cells 120 (2014) 197–203

Contents lists available at ScienceDirect

Solar Energy Materials & Solar Cells

journal homepage: www.elsevier.com/locate/solmat

Simultaneous enhancement in both large-area coatability and photovoltaic performance of inverted organic solar cells with co-solvent

Yun-Ru Hong [a], Pin-Kuan Chen [b], Jen-Chun Wang [c], Ming-Kun Lee [b], Sheng-Fu Horng [b,*], Hsin-Fei Meng [d]

[a] Institute of Photonics Technologies, National Tsing Hua University, Hsinchu 300, Taiwan
[b] Department of Electrical Engineering, National Tsing Hua University, Hsinchu 300, Taiwan
[c] Department of Materials Science and Engineering, National Tsing Hua University, Hsinchu, 30013, Taiwan
[d] Institute of Physics, National Chiao Tung University, Hsinchu, 30013, Taiwan

ARTICLE INFO

Article history:
Received 24 March 2013
Received in revised form
29 August 2013
Accepted 4 September 2013
Available online 16 October 2013

Keywords:
Large area manufacturing
Organic solar cells
Co-solvent
Blade coating
Light soaking

ABSTRACT

We report our observation of simultaneous enhancement in large-area coatability and photovoltaic performance for blade-coated inverted P3HT:PCBM organic solar cells with DCB:hexane co-solvent. The addition of hexane improves greatly the wettability of P3HT:PCBM blend layer on Cs_2CO_3 treated ITO and leads to excessively higher P3HT surface concentration due to the incongruent evaporation of hexane and DCB. A post-processing light soaking was found to further improve the photovoltaic performance for blade-coated devices prepared with co-solvent by adjusting the P3HT surface concentration ratio for more favorable carrier transport, as evidenced by the disappearance of current suppression at forward bias and significant increase in V_{oc} after light soaking. Since large-area manufacturing is the key to full commercialization of organic solar cells, the use of co-solvent, combined with light soaking, may be crucial for the development of inverted organic solar cells.

1. Introduction

Organic solar cell (OSC) is a very promising alternative for solar energy conversion due to their unique and attractive features of low-cost manufacturing, mechanical flexibility, light weight and fabrication feasibility [1–4]. Much progress on OSC has been made with impressive power conversion efficiency and the highest power conversion efficiency (PCE) reported exceeds 10.7% to date [5].

The key property which makes OSCs so attractive is the potential of roll-to-roll processing on low-cost substrates with standard coating and printing processes. This requires large-area high-quality coatings of organic semiconductors. Most of the reported efficient polymer solar cells are fabricated by spin coating technique because of its better control over the thickness and homogeneity of films. However, spin coating is unfavorable for large-area devices, inherently wasteful in material use and is incompatible with roll-to-roll process for high throughput production. To overcome these drawbacks of spin coating process, alternative techniques such as blade coating, slot-die coating, gravure coating, ink-jet printing and spray coating were developed [6–12]. High-throughput continuous processing is crucial for OSCs to manufacture at sufficiently low cost to compete with other thin film solar cell technologies [12–19]. Krebs et al. developed full roll-to-roll processed polymer solar cell modules with a total active area of 35.5 cm^2 and the module PCE achieved 2.75% [20]. Recently, a module with 16 cm^2 aperture area and an efficiency as high as 5.5% was reported by Imec and Solvay [21]. An extensive survey of roll-to-roll technologies for various organic devices, organic solar cells included, by Søndergaard et al., can be found in Ref. [22].

To achieve full commercialization of OSCs, these continuous coating processes need to be carefully studied and various coating defects must be carefully controlled. Coating defects are mainly related to surface tension as well as surface flow and various additives or co-solvents may be used to match the surface tension to reduce the formation of coating defects. In spite of abundant work done in this regard in paint and compliant coating technologies [23,24], there is still little discussion of control over coating defects specifically for OSCs. This is especially important since change in solvent or additives to circumvent the coating defects may affect either the active layer/electrode interface [25] or the distribution and micro-morphology of donor–acceptor in the active layer and thus its photovoltaic properties.

* Corresponding author. Tel.: +886 3 574 2578; fax: +886 3 575 2120.
E-mail address: sfhorng@ee.nthu.edu.tw (S.-F. Horng).

0927-0248/$ - see front matter © 2013 Elsevier B.V. All rights reserved.
http://dx.doi.org/10.1016/j.solmat.2013.09.002

Various types of co-solvents and additives have been proposed for use to improve the efficiency of organic solar cell in the literatures [26–28]; however, most of these previous work focused mainly on their effects on donor/acceptor phase separation. The effects of co-solvents on the film formation in large-area coating processes were little addressed. Schrödner et al. discussed recently the choice of solvent to optimize the photovoltaic performance of organic solar cells manufactured by roll-to-roll slot-die coating and found that $CHCl_3$:DCB mixture can be effectively used to produce efficient large-area OSCs, yet only conventional OSCs are examined [29].

In this paper, we report our observation that the use of 1,2-dichlorobenzene:n-hexane (DCB:hexane) co-solvent can improve both the film formation in large-area coating process and the photovoltaic performance of the resulted inverted organic solar cells. X-Ray photoelectron spectroscopy (XPS) results reveal that the addition of hexane in the solution results in excessive increase in P3HT compositional ratio on the surface due to the incongruent evaporation of hexane and DCB. After a post-processing light soaking for 40 min with an AM 1.5G solar simulator, the PCE of the blade-coated inverted OSCs reaches 3.92%, thus demonstrating the possibility of simultaneous enhancement in both large-area manufacturability and photovoltaic performance for inverted OSCs.

2. Experiment

The schematic diagram of the device structure of OSC considered in this study is shown in Fig. 1. The devices were prepared as follows. Indium tin oxide (ITO) coated glass was cleaned by acetone, isopropanol (IPA) and de-ionized water for 10 min, respectively to remove residual organic materials. An electron transport material, 0.1 wt% Cs_2CO_3 (99%, purchased from ALFA, Inc.) dissolved in 2-ethoxyethanol, was blade-coated on the prepared ITO-coated substrates with coating speed of 20 mm/s and then dehydrated at 150 °C for 10 min. Two types of solvents for the blend layer of OSC were investigated in this work. The first is DCB and the other is a co-solvent consisting of DCB:hexane in 1:1 volume ratio. The blend solution was prepared by mixing P3HT (17 mg ml^{-1}, purchased from Rieke Metals, Inc.) and PCBM (17 mg ml^{-1}, purchased from Nano-C, Inc.) in either DCB or the co-solvent. Each blend solution was blade-coated on the Cs_2CO_3-coated ITO substrate with typical coating speed of 13.3 mm/s and was subsequently annealed at 140 °C for 10 min. The area of ITO-coated glass substrate used to study large-area coatability was 7 cm by 8 cm. Two types of small-area solar cells with active area of 4 mm^2 (Device A and B) were fabricated to investigate the effects of co-solvent on photovoltaic performance. Both were prepared following the same fabrication steps except for the preparation of blend solution. For Device A, the aforementioned blend solution prepared with DCB was used and for Device B, the blend solution with co-solvent. Each blend solution was blade-coated on the Cs_2CO_3-coated ITO substrate with coating speed of 13.3 mm/s and annealed at 140 °C for 10 min. PEDOT:PSS (AI 4083, purchased from H. C. Starck, Inc.) solution diluted in IPA with the weight ratio of 1:10 (AI 4083:IPA) was blade-coated on top of the blend layer with the coating speed of 13.3 mm/s and was then annealed at 140 °C for 10 min. The doctor blade used in this study is purchased from Elcometer Co. Ltd. (model 3520) and is motorized by a linear motor system (model LMX1L-S, HIWIN Co. Ltd.). A photo of the coating system was shown in Fig. 2. The details of the setup of the blade coating system can be found in Ref. [30]. The polymer wet film was obtained by dragging the deposited solution with the coating blade and the solution concentration of polymer, the blade's speed and the gap between the doctor blade and the substrate determine the thickness of polymer films. In this work, 60 μm gap was employed for the Cs_2CO_3 as well as blend layers, and 30 μm gap was used for the diluted PEDOT:PSS. The thickness of various layers was measured by an Alpha Step Profilier (model. Alpha step 500, Tencor Inc.) For the small-area device, the thickness after annealing is 220($\pm$20) nm for the blend layer with both DCB and co-solvent, and 40($\pm$5) nm for PEDOT:PSS. Subsequently, a top metal electrode of Silver (100 nm) was thermally deposited under a pressure of 2.3×10^{-6} Torr. The fabricated

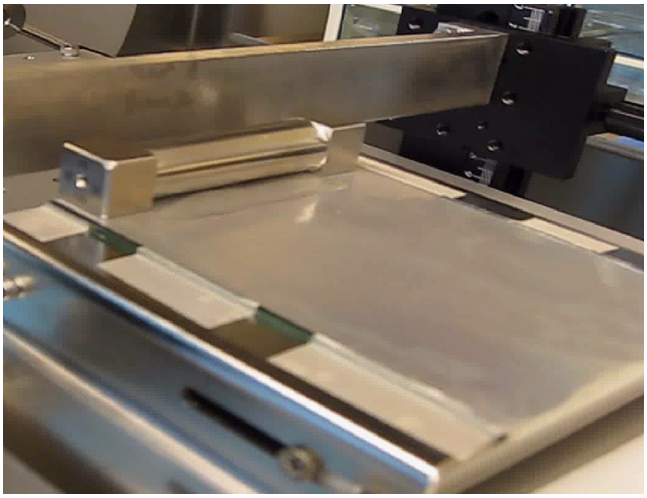

Fig. 2. The picture of the coating system, consisting of a doctor blade motorized by a linear motor system and home-made supporting stage.

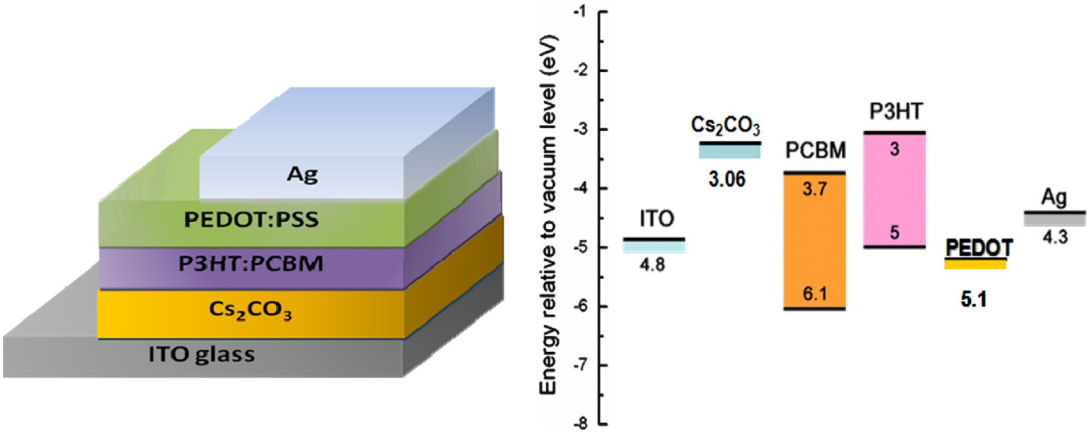

Fig. 1. (a) The device structure and (b) the energy band diagram of the inverted organic solar cell investigated in the present study.

devices were encapsulated using a UV-cured sealant and a cover glass under nitrogen ambient.

3. Characterization

The current density–voltage (*J–V*) characteristics of the devices were measured by Keithley 2400 source measurement unit using a 100 mW cm^{-2} AM 1.5G solar simulator (San-Ei Electric, XES 301S). The intensity of the incident solar illumination was calibrated by a silicon photodiode (HAMAMATSU S1337-BR). The same solar simulator was used for post-processing continuous light soaking illumination which we found to enhance the device photovoltaic performance [31]. The external quantum efficiency (EQE) was conducted using a measurement system (model QE-R) built by Enli Technology Co. Ltd. Wide-spectrum light source is chopped and diffracted into separated monochromatic narrow bands, and each of which is projected onto the device under testing. The photo-current generated by incident monochromatic light was converted and amplified to an AC voltage by a trans-impedance amplifier, which was then measured by a DAQ card at the chopper frequency. Surface roughness and morphology of the blend films were estimated by Atomic force microscopy (AFM) images (Veeco Nanoscope). The XPS measurements were conducted inside an ultrahigh vacuum system (Thermo Microlab 350). The XPS spectra were measured utilizing Mg Ka (1253.6 eV) X-ray source for the surface composition of the blend layers. The contact angles were measured using a video-based optical contact angle meter (Model 100SE, Sindatek Co. Ltd.).

4. Results and discussion

Fig. 3(a) and (b) show the images of blade-coated blend layers prepared with DCB and DCB:hexane co-solvent, respectively. While the blend layer prepared with DCB exhibits clearly "orange peel" defects, the surface of co-solvent prepared blend layer is found to be smooth and defect-free. With co-solvent and the coating parameters we used, the thickness of the blend layer prepared after annealing is 220($\pm$20) nm across an area of 7 cm by 8 cm. This improvement of surface morphology can be understood by noting that the addition of hexane to DCB reduces the surface tension as well as viscosity and enhance the film leveling and the wettability between the solvent and Cs_2CO_3. Fig. 4(a) and (b) show the results of contact angle measurements of DCB and DCB:hexane co-solvent in 10:1 volume ratio, both on Cs_2CO_3 treated ITO. The equilibrium contact angle was found to decrease from 22° in the case of pure DCB to 8.5° for the co-solvent with merely 10% addition of hexane. For the case of 1:1 DCB:hexane co-solvent we used for our blade coating, the contact angle is too small to determine, revealing greatly improved wettability between the co-solvent and the Cs_2CO_3 treated ITO.

AFM measurement was used to investigate the effects of solvent on surface micro-morphology of blend films. Fig. 5 (a)–(d) show the AFM topographic and phase images of the blend surface prepared with pure DCB and DCB:hexane co-solvent, respectively. From Fig. 5(a) and (b), finer aggregation and smaller root-mean-square surface roughness (8.3 nm) were observed from the blend surface prepared with co-solvent than that with pure DCB (13.2 nm). Moreover, the phase images of the co-solvent prepared blend surface (Fig. 5(c)) exhibit less contrast and thus more segregated P3HT on the surface than that with DCB (Fig. 5(d)).

The absorption of the blend layers prepared with DCB and DCB: hexane co-solvent was measured and the results were shown in Fig. 6. Although the thickness of both blend layers was specially chosen to be identical (200 nm), the film prepared with co-solvent exhibits more absorption than that with DCB. We speculate that this enhanced absorption of the co-solvent prepared blend layer may be explained by the better self-organizing of the segregated P3HT into highly ordered structure, which was observed to lead to increase in absorption [32].

To investigate the effects of co-solvent on the device photovoltaic performance without involving complication due to structural non uniformity present in large area cells, small-area devices were prepared and characterized. The measured dark and the illuminated *J–V* curves of as-prepared devices with pure DCB (device A) and with co-solvent (device B) are shown in Fig. 7(a). As compared to device A, device B exhibits enhanced V_{oc}, J_{sc}, fill factor and thus PCE. Therefore, compared to DCB, the use of DCB: hexane solvent improves simultaneously the photovoltaic performance and the large-area coatability of inverted organic solar cells.

It is interesting to note from Fig. 7(a) that, while device A exhibits conventional diode-like dark and illuminated *J–V* curves, both the dark and illuminated *J–V* curves of device B show current suppression at forward bias higher than V_{oc}, revealing retarded transport of the injected carriers from the electrodes into the device. Similar current suppression at forward bias was previously observed for as-prepared inverted OSCs and was found to revert normal diode-like with a post-processing light soaking [31,33]. Both device A and device B were thus subject to a continuous light soaking under the same AM 1.5G solar simulator for 40 min. The *J–V* curves measured after the light soaking are shown in Fig. 7(b) and the photovoltaic parameters for both devices before

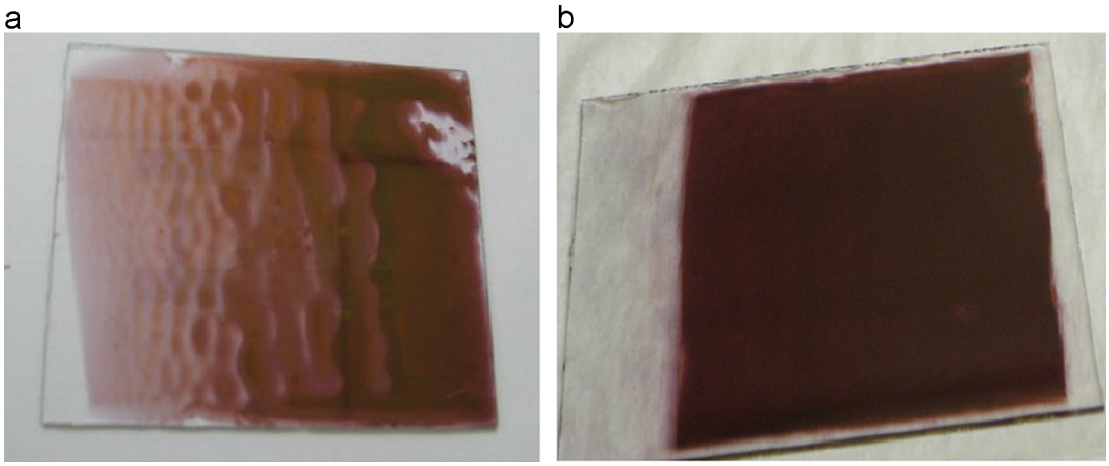

Fig. 3. The pictures of large-area blend layers prepared by blade coating with (a) DCB and (b) DCB:hexane co-solvent. The size of the substrates is 7 cm by 8 cm.

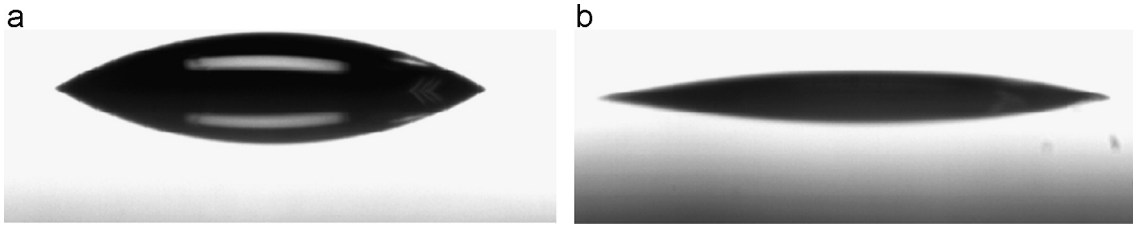

Fig. 4. Images of contact angle measurements of (a) DCB and (b) DCB:hexane co-solvent in 10:1 volume ratio on Cs_2CO_3 treated ITO.

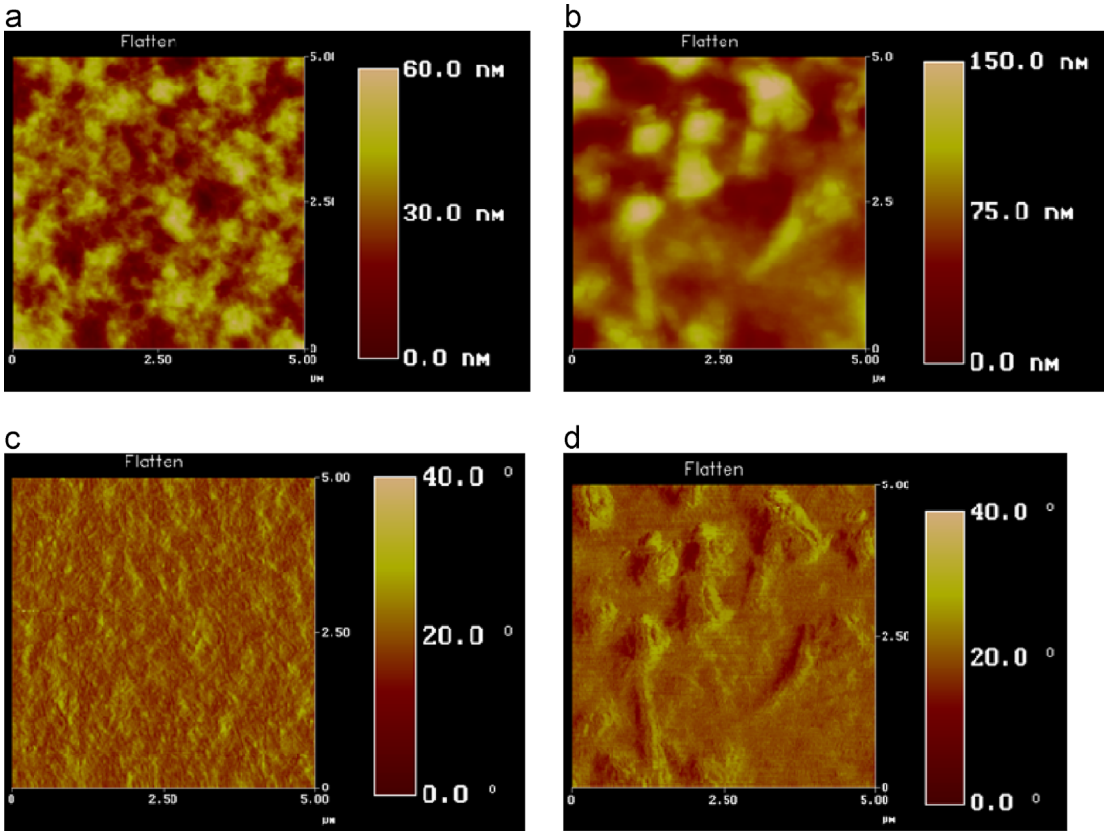

Fig. 5. The AFM topographic images of the P3HT/PCBM blend layer surface prepared with (a) co-solvent and (b) DCB. (c) and (d) are the corresponding phase images. The size of the scanned area is 5 μm by 5 μm.

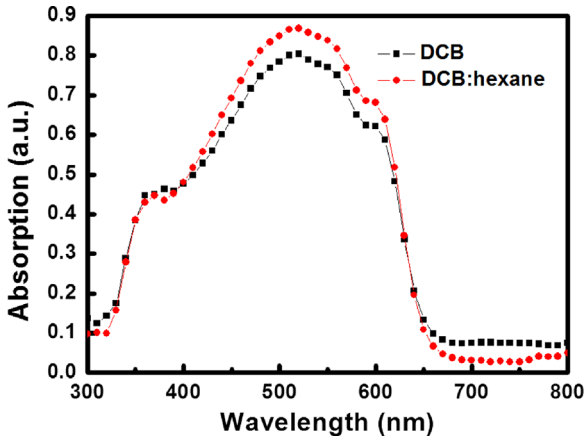

Fig. 6. The absorption spectra for blend layer prepared with DCB and co-solvent, respectively.

and after light soaking are summarized in Table 1. After light soaking, the current suppression at forward bias observed from device B disappears and both the dark and illuminated *J–V* curve exhibit normal diode-like characteristics. This enhancement in photovoltaic performance and disappearance of current suppression with light soaking are similar to observation previously reported from inverted organic solar cells with ZnO electron-selective layer [31,33,34]. In our cases, enhancement in photovoltaic performance was observed for both device A and B. The PCE increases from 2.2% (2.96%) for the as-prepared device to 3.03% (3.92%) with light soaking for device A (device B). From Table 1, it is also remarkable that while the improvement for device A is mostly due to increase in J_{sc} (from 9.21 to 10.31 mA/cm^2), the enhancement for device B results dominantly from increase in V_{oc} (from 0.57 to 0.64 V). The significant increase in V_{oc} with light soaking for device B is similar to what was previously observed [31].

The absorption of the blend layers after light soaking was measured and was found to remain unchanged from that obtained before the light soaking process (Fig. 6). Fig. 8(a) and (b) show the EQE of the devices prepared with DCB and co-solvent before and after light soaking. Similar to what was reported previously light soaking enhances the photovoltaic performance for both devices. Since the absorption of active layer does not change, increased EQE indicates improved carrier transport and carrier collection efficiency with light soaking.

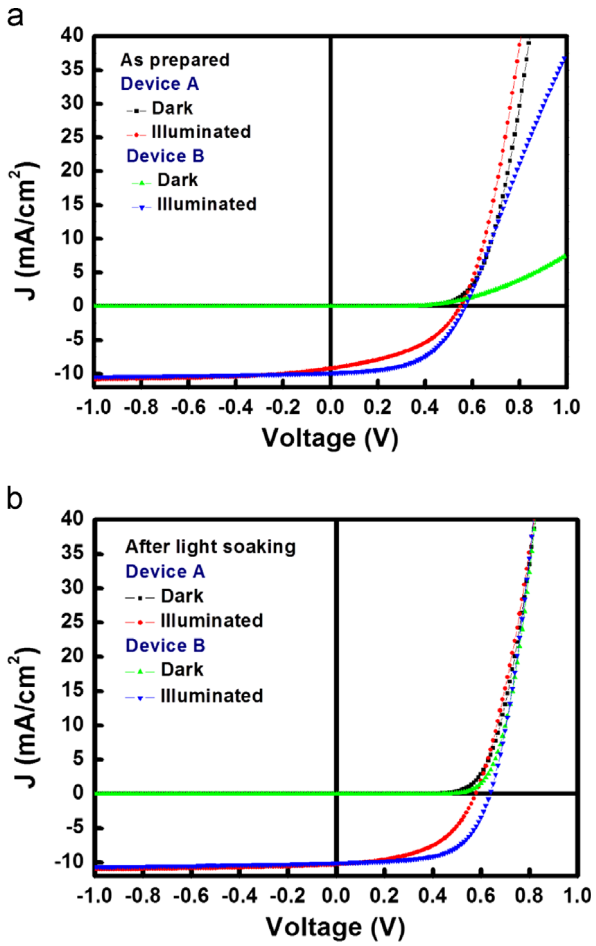

Fig. 7. Measured dark and illuminated *J–V* curves for inverted OSCs prepared with DCB (Device A) and DCB:hexane (Device B) (a) before and (b) after light soaking (b) The illuminated *J–V* characteristics of the as-prepared and light-soaked inverted organic solar cells under illumination.

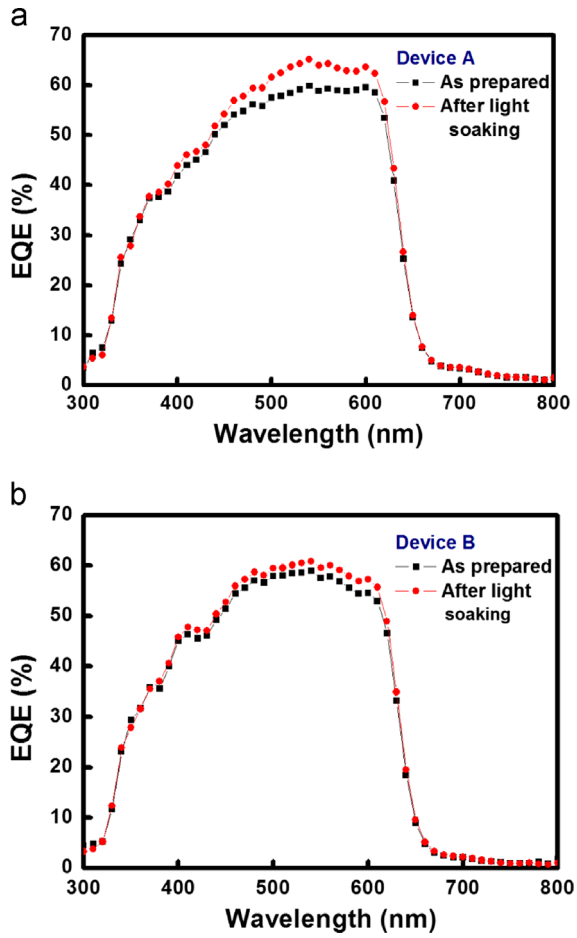

Fig. 8. The EQE spectra of the devices prepared with (a) DCB and (b) co-solvent before and after light soaking.

Table 1
Summary of the photovoltaic parameters of inverted OSCs prepared with DCB and DCB:hexane co-solvent before and after light soaking. 100 mW/cm^2 AM1.5G simulated solar illumination is used for the characterization.

		J_{sc} (mA/cm^2)	V_{oc} (V)	Fill factor (%)	PCE (%)
DCB	As prepared	9.21	0.55	0.43	2.20
	After light soaking	10.31	0.58	0.51	3.03
DCB:hexane	As prepared	9.86	0.57	0.53	2.96
	After light soaking	10.06	0.64	0.61	3.92

XPS was employed to characterize the surface composition of blend layers prepared with DCB and co-solvent. The samples for XPS characterization were prepared in the same way as described previously except that they were not covered with PEDOT:PSS and metal electrode. These samples were encapsulated with glass and half of them were subject to continuous light soaking for 40 min. The glass covers of the samples were detached immediately before loading into the XPS chamber. Sulfur (S) 2p and carbon (C) 1s signals were detected. Thermo Avantage software (v3.20) was used to calculate the S to C atomic ratios, which in turn were transformed to P3HT to PCBM relative weight percentage. The measured S 2p core levels were shown in Fig. 9 and the calculated results were summarized in Table 2.

From Table 2, the P3HT weight ratios on the surface are 89.89% and 94.37% for as-prepared blend layer with DCB and co-solvent, respectively. These are much higher than those previously

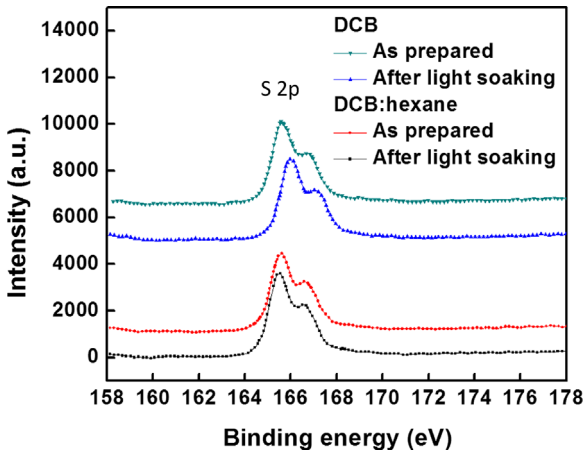

Fig. 9. The XPS spectra of S 2p core level obtained from the surface of P3HT/PCBM blend layers prepared with different solvents before and after light soaking.

observed from the blend layers prepared with spin coating process [35–37]. High P3HT surface concentrations can be attributed to the blade coating process with which there is sufficient drying time to permit of vertical concentration segregation. Higher P3HT surface concentration for blend layer with co-solvent than DCB can be understood by noting that the addition of hexane increases the solubility of PCBM in the co-solvent because of better matched solubility parameters (Table 3) [38–40]. Since the boiling points of hexane (68.7 °C) is lower than that of DCB (180.5 °C) and the blade coating process allows for sufficient drying time, hexane

Table 2
Atomic and weight ratios of the surface composition in P3HT/PCBM blend layers prepared with different solvents before and after light soaking.

		Atom (%)		Weight (%)	
		C 1S	S 2P	PCBM	P3HT
DCB	As prepared	91.98	8.02	10.11	89.89
	After light soaking	91.73	8.27	7.72	92.28
DCB:hexane	As prepared	91.51	8.49	5.63	94.37
	After light soaking	91.59	8.41	6.38	93.62

Table 3
Solubility parameters of solutes and solvents used in this study.

Solvent or solute	Solubility parameter δ $(J/cm^3)^{1/2}$
DCB	20.5
hexane	14.9
PCBM	7.8
P3HT	19.42
DCB:hexane	17.7

evaporates incongruently from the surface of the resulted blend layers. As a result the PCBM near the surface will tend to diffuse to the lower stratum of the blend layer which contains more hexane, leading to higher P3HT surface concentration than that prepared with DCB. Higher P3HT surface composition ratio for blade-coated sample prepared with co-solvent than DCB is also consistent with the AFM phase image (Fig. 5(c) and (d)), in which less phase contrast and thus more segregated P3HT on the surface of co-solvent prepared layer was observed.

After the light soaking, the P3HT surface concentration for the blend layer prepared with DCB increases to 92.28%. On the other hand, it decreases from 94.37% to 93.62% for the blend layer prepared with co-solvent. Since both devices shows improved carrier transport and carrier collection efficiency with light soaking (Fig. 8), our results suggest that there is an optimum degree of vertical concentration segregation for inverted organic solar cells. For device A prepared with DCB with less vertical concentration segregation than the optimal value, which corresponds to a P3HT surface composition ratio around 92–93%, post-processing light soaking enhances the vertical segregation and improves the carrier transport [31]. On the other hand, for as prepared device B, the excessively segregated P3HT (PCBM) at the blend/anode (blend/cathode) interface may impede the transport of electrons (holes) to the anode (cathode) and leads to carrier accumulation at the blend/electrode interfaces which screens bulk electric field within the device, resulting in reduced carrier collection efficiency. This may also explain the current suppression at forward bias higher than V_{oc} for as prepared device B. Light soaking seems to reduce the extent of vertical segregation and improve the carrier transport and collection. As a result, the current suppression observed at forward bias disappears (Fig. 7) and V_{oc} increases significantly (Table 1) after the light soaking.

5. Conclusion

In summary, DCB:hexane co-solvent was found to enhance greatly the large-area coatability of blade-coated P3HT:PCBM blend layer on Cs_2CO_3 treated ITO due to improved wettability. Compared to commonly used DCB, co-solvent prepared P3HT:PCBM inverted organic solar cells also show enhanced photovoltaic performance. The blade-coated blend layer prepared with co-solvent exhibits excessively high P3HT surface concentration due to the incongruent evaporation of hexane and DCB. A post-processing light soaking for 40 min with an AM 1.5G solar simulator was found to further improve the photovoltaic performance of the blade-coated devices prepared respectively with DCB and DCB:hexane co-solvent by adjusting the vertical segregation for more favorable carrier transport. The use of DCB:hexane co-solvent, combined with light soaking, can thus be useful for large-area manufacturing of inverted organic solar cells.

Acknowledgment

This work was supported by the National Science Council (NSC) of Taiwan, the Republic of China, under grant NSC 100–2221-E-007–079-MY3.

References

[1] F.C. Krebs, Fabrication and processing of polymer solar cells: a review of printing and coating techniques, Solar Energy Materials and Solar Cells 93 (2009) 394–412.
[2] C.N. Hoth, S.A. Choulis, P. Schilinsky, C.J. Brabec, On the effect of poly (3-hexylthiophene) regioregularity on inkjet printed organic solar cells, Journal of Materials Chemistry 19 (2009) 5398.
[3] Y. Liang, Z. Xu, J. Xia, S.T. Tsai, Y. Wu, G. Li, C. Ray, L. Yu, For the bright future-bulk heterojunction polymer solar cells with power conversion efficiency of 7.4%, Advanced Materials 22 (2010) E135–E138.
[4] B.C. Thompson, J.M.J. Frechet, Polymer–fullerene composite solar cells, Angewandte Chemie International Edition 47 (2008) 58–77.
[5] ⟨http://www.heliatek.com/⟩.
[6] F.C. Krebs, M. Jørgensen, K. Norrman, O. Hagemann, J. Alstrup, T.D. Nielsen, J. Fyenbo, K. Larsen, J. Kristensen, A complete process for production of flexible large area polymer solar cells entirely using screen printing-first public demonstration, Solar Energy Materials and Solar Cells 93 (2009) 422–441.
[7] Y.H. Chang, S.R. Tseng, C.Y. Chen, H.F. Meng, E.C. Chen, S.F. Horng, C.S. Hsu, Polymer solar cell by blade coating, Organic Electronics 10 (2009) 741–746.
[8] F. Padinger, C.J. Brabec, T. Fromherz, J.C. Hummelen, N.S. Sariciftci, Fabrication of large area photovoltaic devices containing various blends of polymer and fullerene derivatives by using the doctor blade technique, Opto-Electronics Review 8 (2000) 280–283.
[9] W.B. Byun, S.K. Lee, J.C. Lee, S.J. Moon, W.S. Shin, Bladed organic photovoltaic cells, Current Applied Physics 11 (2011) S179–S184.
[10] M.M. Voigt, R.C.I. Mackenzie, S.P. King, C.P. Yau, P. Atienzar, J. Dane, P.E. Keivanidis, I. Zadrazil, D.D.C. Bradley, J. Nelson, Gravure printing inverted organic solar cells: The influence of ink properties on film quality and device performance, Solar Energy Materials and Solar Cells 105 (2012) 77–85.
[11] J.W. Kang, Y.J. Kang, S. Jung, D.S. You, M. Song, C.S. Kim, D.G. Kim, J.K. Kim, S. H. Kim, All-spray-coated semitransparent inverted organic solar cells: from electron selective to anode layers, Organic Electronics 13 (2012) 2940–2944.
[12] F.C. Krebs, Polymer solar cell modules prepared using roll-to-roll methods: knife-over-edge coating, slot-die coating and screen printing, Solar Energy Materials and Solar Cells 93 (2009) 465–475.
[13] C. Lungenschmied, G. Dennler, H. Neugebauer, S.N. Sariciftci, M. Glatthaar, T. Meyer, A. Meyer, Flexible, long-lived, large-area, organic solar cells, Solar Energy Materials and Solar Cells 91 (2007) 379–384.
[14] L. Blankenburg, K. Schultheis, H. Schache, S. Sensfuss, M. Schrodner, Reel-to-reel wet coating as an efficient up-scaling technique for the production of bulk-heterojunction polymer solar cell, Solar Energy Materials and Solar Cells 93 (2009) 476–483.
[15] C.N. Hoth, P. Schilinsky, S.A. Choulis, C.J. Brabec, Printing highly efficient organic solar cells, Nano Letters 8 (2008) 2806–2813.
[16] M. Manceau, D. Angmo, M. Jørgensen, F.C. Krebs, ITO-free flexible polymer solar cells: From small model devices to roll-to-roll processed large modules, Organic Electronics 12 (2011) 566–574.
[17] F.C. Krebs, S.A. Gevorgyan, J. Alstrup, A roll-to-roll process to flexible polymer solar cells: model studies, manufacture and operational stability studies, Journal of Materials Chemistry 19 (2009) 5442–5451.
[18] F.C. Krebs, T. Tromholt, M. Jørgensen, Upscaling of polymer solar cell fabrication using full roll-to-roll processing, Nanoscale 2 (2010) 873–886.
[19] F.C. Krebs, Roll-to-roll fabrication of monolithic large-area polymer solar cells free from indium-tin-oxide, Solar Energy Materials and Solar Cells 93 (2009) 1636–1641.
[20] F.C. Krebs, J. Fyenbo, M. Jørgensen, Product integration of compact roll-to-roll processed polymer solar cell modules: methods and manufacture using flexographic printing, slot-die coating and rotary screen printing, Journal of Materials Chemistry 20 (2010) 8994–9001.
[21] ⟨http://www.imec.org/index.cfm⟩.

[22] R.R. Søndergaard, M. Hösel, F.C. Krebs, Roll-to-Roll fabrication of large area functional organic materials, Journal of Polymer Science Part B: Polymer Physics 51 (2013) 16–34.
[23] J. Schwartz, B.A. Moyer, R.E. Smith, Control of film defects in solventborne high-solids coatings: the non-additives vs. a new additives approach, Journal of Coatings Technology 70 (1998) 71–78.
[24] A. Abbasian, S.R. Ghaffarian, N. Mohammadi, M.R. Khosroshahi, M. Fathollahi, Study on different planforms of paint's solvents and the effect of surfactants, Progress in Organic Coatings 49 (2004) 229–235.
[25] M. Graetzel, R.A.J. Janssen, D.B. Mitzi, E.H. Sargent, Materials interface engineering for solution-processed photovoltaics, Nature 488 (2012) 304–312.
[26] N.E. Coates, I.W. Hwang, J. Peet, G.C. Bazan, D. Moses, A.J. Heeger, 1,8-octanedithiol as a processing additive for bulk heterojunction materials: enhanced photoconductive response, Applied Physics Letters 93 (2008) 072105.
[27] Y. Yao, J. Hou, Z. Xu, G. Li, Y. Yang, Effects of solvent mixtures on the nanoscale phase separation in polymer solar cells, Advanced Functional Materials 18 (2008) 1783–1789.
[28] S.H. Jin, B.V.K. Naidu, H.S. Jeon, S.M. Park, J.S. Park, S.C. Kim, J.W. Lee, Y.S. Gal, Optimization of process parameters for high-efficiency polymer photovoltaic devices based on P3HT:PCBM system, Solar Energy Materials and Solar Cells 91 (2007) 1187–1193.
[29] M. Schrödner, S. Sensfuss, H. Schache, K. Schultheis, T. Welzel, K. Heinemann, R. Milker, J. Marten, L. Blankenburg, Reel-to-reel wet coating by variation of solvents and compounds of photoactive inks for polymer solar cell production, Solar Energy Materials and Solar Cells 107 (2012) 283–291.
[30] C.Y. Chen, H.W. Chang, Y.F. Chang, B.J. Chang, Y.S. Lin, Continuous blade coating for multi-layer large-area organic light-emitting diode and solar cell, Journal of Applied Physics 110 (2011) 094501.
[31] J.C. Wang, C.Y. Lu, J.L. Hsu, M.K. Lee, Y.R. Hong, T.P. Perng, S.F. Horng, H.F. Meng, Efficient inverted organic solar cells without an electron selective layer, Journal of Materials Chemistry 21 (2011) 5723–5728.
[32] C.W. Liang, W.F. Su, L. Wang, Enhancing the photocurrent in poly(3-hexylthiophene)/[6,6]-phenyl C61 butyric acid methyl ester bulk heterojunction solar cells by using poly(3-hexylthiophene) as a buffer layer, Apply Physics Letters 95 (2009) 133303.
[33] M.R. Lilliedal, A.J. Medford, M.V. Madsen, K. Norrman, F.C. Krebs, The effect of post-processing treatments on inflection points in current–voltage curves of roll-to-roll processed polymer photovoltaics, Solar Energy Materials and Solar Cells 94 (2010) 2018–2031.
[34] J. Gilot, M.M. Wienk, R.A. Janssen, Double and triple junction polymer solar cells processed from solution, Applied Physics Letters 90 (2007) 143512.
[35] J.S. Kim, P.K.H. Ho, C.E. Murphy, R.H. Friend, Phase separation in polyfluorene-based conjugated polymer blends: lateral and vertical analysis of blend spin-cast thin films, Macromolecules 37 (2004) 2861–2871.
[36] K.H. Yim, Z. Zheng, Z. Liang, R.H. Friend, W.T.S. Huck, J.S. Kim, Efficient conjugated-polymer optoelectronic devices fabricated by thin-film transfer-printing technique, Advanced Functional Materials 18 (2008) 1012–1019.
[37] Z. Xu, L.M. Chen, G. Yang, C.H. Huang, J. Hou, Y. Wu, G. Li, C.S. Hsu, Y. Yang, Vertical phase separation in poly(3-hexylthiophene):fullerene derivative blends and its advantage for inverted structure solar cells, Advanced Functional Materials 19 (2009) 1227–1234.
[38] T. Salim, L.H. Wong, B. Bräuer, R. Kukreja, Y.L. Foo, Z. Bao, Y.M. Lam, Solvent additives and their effects on blend morphologies of bulk heterojunctions, Journal of Materials Chemistry 21 (2011) 242–250.
[39] L. Xue, X. Gao, K. Zhao, J. Liu, X. Yu, Y. Han, The formation of different structures of poly(3-hexylthiophene) film on a patterned substrate by dip coating from aged solution, Nanotechnology 21 (2010) 145303.
[40] J. Brandrup, E.H. Immergut, E.A. Grulke, Polymer Handbook, 2nd ed., John Wiley & Sons, New York, 1999.